Article

Assessment of Seasonal Energy Efficiency Strategies of a Double Skin Façade in a Monsoon Climate Region

Taehoon Hong *, Jimin Kim, Juyoung Lee, Choongwan Koo and Hyo Seon Park

Department of Architectural Engineering, Yonsei University, Seoul 120-749, Korea;
E-Mails: cookie6249@yonsei.ac.kr (J.K.); kevinlee2080@yonsei.ac.kr (J.L.);
cwkoo@yonsei.ac.kr (C.K.); hspark@yonsei.ac.kr (H.S.P.)

* Author to whom correspondence should be addressed; E-Mail: hong7@yonsei.ac.kr;
Tel.: +82-2-2123-5788; Fax: +82-2-2248-0382.

Abstract: As climate change and global warming have become two of the most significant environmental issues today, the double-skin façade (DSF) is getting considerable attention as an energy-efficient passive design. This study is aimed at assessing the seasonal energy efficiency strategies of a DSF targeting library facilities in the climate region with hot summers and cold winters. Toward this end, this study was conducted in four steps: (i) establishment of seasonal energy-efficient strategies; (ii) application of seasonal energy-efficient strategies; (iii) analysis of energy saving effect by season; and (iv) life cycle cost and life cycle CO_2 analyses for selecting an optimal DSF. Results show that a shaft box DSF energy model (EM_S) #2, which applied winter strategies, was optimal with an energy saving rate of 4.13%, while a multi-story DSF energy model (EM_M) #5, which applied summer strategies, was optimal with an energy saving rate of 12.67%. In terms of savings to investment ratio (SIR_{40}) and breakeven point (BEP_{40}), the multi-story DSF (3.20; 9 years) was superior. The results of this study can be used for (i) seasonal energy efficiency strategies of a DSF in East Asian monsoon climates, and (ii) as a guideline for the application of a DSF both in existing and new buildings.

Keywords: double skin façade (DSF); airflow operating method; thermal insulation; green wall; energy-saving effect; life cycle cost; life cycle CO_2; East Asian monsoon climate; library facility

1. Introduction

The recent increase in global energy consumption has led to a phenomenon called global warming and related climate problems, resulting in a growing interest in developing various technologies that aim to reduce energy consumption, including passive designs, which can reduce the energy load of a building [1,2]. Though unrelated to various efforts in reducing energy consumption, the ratio of glazing in building façades has also increased for aesthetic purposes. As a result, direct solar radiation inside the building rose, causing thermal issues as well as increased heating and cooling energy consumption. Particularly, in hot climate regions, the energy cost attributed to the increase in cooling energy consumption significantly increased [3–6]. To solve these issues, various energy saving techniques have been introduced to block direct solar radiation, such as tinted glass, colored glass and phase changing materials. In particular, there is a growing interest in the double skin façade (DSF), which can be implemented in buildings with a high glazing ratio [7,8].

A DSF consists of the external and inner skins, as well as the cavity existing between the two skins. Since the heat transfer on DSF occurs due to the temperature differences among the external skin, cavity, and the inner skin of a building, managing the heat in the cavity in the summer and in the winter is a key issue. Thus, research on: (i) the shading and the airflow operating methods in the cavity and (ii) the thermal insulation of the glass and the inner skin in the cavity have been conducted. Research on thermal management in the cavity of DSF can be categorized into two types: (i) heating and cooling energy reduction by implementing airflow operating methods; and (ii) thermal bridge effect reduction by improving thermal insulation.

First, several studies have focused on the airflow operating methods by opening and shutting the openings in the cavity of DSF. In winter, the heat in the cavity can considerably reduce the heating load of a building in terms of thermal comfort. Particularly, in winter, conducting the heat in the cavity to the building's interior can be maximized by using a static air buffer as an airflow operating method, which seals the heat in the cavity [9–12]. The Telus Headquarters building in Toronto and the Occidental Chemical buildings in Niagara Falls and in New York use a static air buffer as an airflow operating method to reduce heating energy consumption in winter [13]. Additionally, Xu *et al.* [14] analyzed that 20% to 30% of heating energy consumption can be reduced by using a static air buffer in applying DSF to buildings in Japan. Gracia *et al.* [15] also showed that the static air buffer could save up to 26% of heating energy consumption in winter. Next, the cooling load on a building can increase in the summer because of the heated air in the cavity [16–18]. Accordingly, in terms of thermal comfort, management of heated air in the cavity in summer is an important issue. Various studies have been conducted on the airflow operating methods in implemented during summertime. It has been shown that the external air curtain as an airflow operating method that opens the openings in the cavity (*i.e.*, allowing the heat in the cavity to travel freely outside) would save cooling energy consumption during summer because the heated air in the cavity due to solar radiation could be removed in advance before being transmitted to a building [9,12–14]. To discharge the heated air in the cavity and the building to outside the building, natural ventilation, as well as the external air curtain, are also considered important [7,18–21]. Gratia *et al.* [21] mentioned the significance of natural ventilation after sunset in addition to the duration of sunshine through solar radiation in summer. By emitting the heat inside the building through natural ventilation, 25.5% of cooling energy consumption was saved [7].

Based on the previous studies related to the airflow operating methods, there was little research that simultaneously applies the airflow operating methods and natural ventilation with the consideration of the climate differences between summer and winter. Therefore, this study focused on the facilities located in the regions with the hot summer and cold winter, simultaneously. The East Asian monsoon climate is divided into a hot and wet summer monsoon and a cold and dry winter monsoon, resulting from the monsoonal flow that carries moist air from the Indian Ocean and Pacific Ocean to East Asia. It is driven by the temperature differences between the Asian continent and the Pacific Ocean. Although the East Asian monsoon climate region (e.g., Seoul) has four seasons including spring and fall, spring and fall only last for a short period in this climate region [22–25], therefore, this study only focused on the climatic characteristics in summer and winter.

Second, as a method of controlling heat in the cavity of DSF, various studies have focused on reducing the thermal bridge effect by improving the thermal insulation of the inner skin. It has been shown that the method was effective in both summer and winter. In terms of the thermal bridge effect, Manz [26] and Perez-Grande *et al.* [27] conducted studies on reducing heating and cooling loads by improving the thermal insulation of the inner skin glazing. Other studies have also shown that improvement in the thermal insulation of the inner wall reduces the thermal bridge effect [16,28–31]. Feist [30] has shown that heating and cooling energy consumption increases due to the unnecessary heat transfer caused by the thermal bridge effect on the wall in addition to the window. Evola *et al.* [31] determined that there is about 3.5% of the increase in cooling energy consumption due to the thermal bridge effect of the building skin during summer.

Other studies have focused on reducing the thermal bridge effect by implementing a green wall (GW) on a single skin façade (SSF) [32–36]. Studies showed that installing a GW on the facades of a two-story building could reduce the cooling load on a clear summer day by 28% [33]. Akbari *et al.* [34] has shown that the installation of a GW would reduce heat transfer by 0.24 kWh/m^2. Likewise, other researchers have shown that the use of plants as shading devices in warm or tropical regions would reduce the cooling load in summer as they helped create a sun-blocking effect [35–38]. These previous studies on thermal bridge effect have concentrated mainly on SSF buildings, while only a few considered DSF buildings. Therefore, this study focused on reducing the thermal bridge effect by implementing GW as the seasonal energy efficiency strategies of a DSF.

In conclusion, it has been shown that in implementing DSF, the management of heat in the cavity is a very important control factor in cooling and heating energy consumption reduction. Therefore, this study aimed to establish seasonal energy efficiency strategies, and evaluate the effect of these strategies to efficiently manage heat in the cavity of DSF. Furthermore, it aimed to implement these seasonal energy efficiency strategies to four types of DSF, and select an optimal DSF after conducting life cycle cost (LCC) and life cycle CO_2 (LCCO$_2$) analyses.

This study was conducted in four steps: (i) establishment of seasonal energy efficiency strategies; (ii) application of seasonal energy efficiency strategies; (iii) analysis of energy saving effect by season by applying seasonal energy efficiency strategies; and (iv) LCC and LCCO$_2$ analyses for selecting an optimal DSF. The scope of this study included library facilities located in Seoul, South Korea, which is part of the East Asian monsoon climate region. As mentioned spring and fall only last for a short period in this climate region, therefore, this study only considered winter and summer characteristics to establish seasonal energy efficiency strategies (Figure 1).

Figure 1. Research framework.
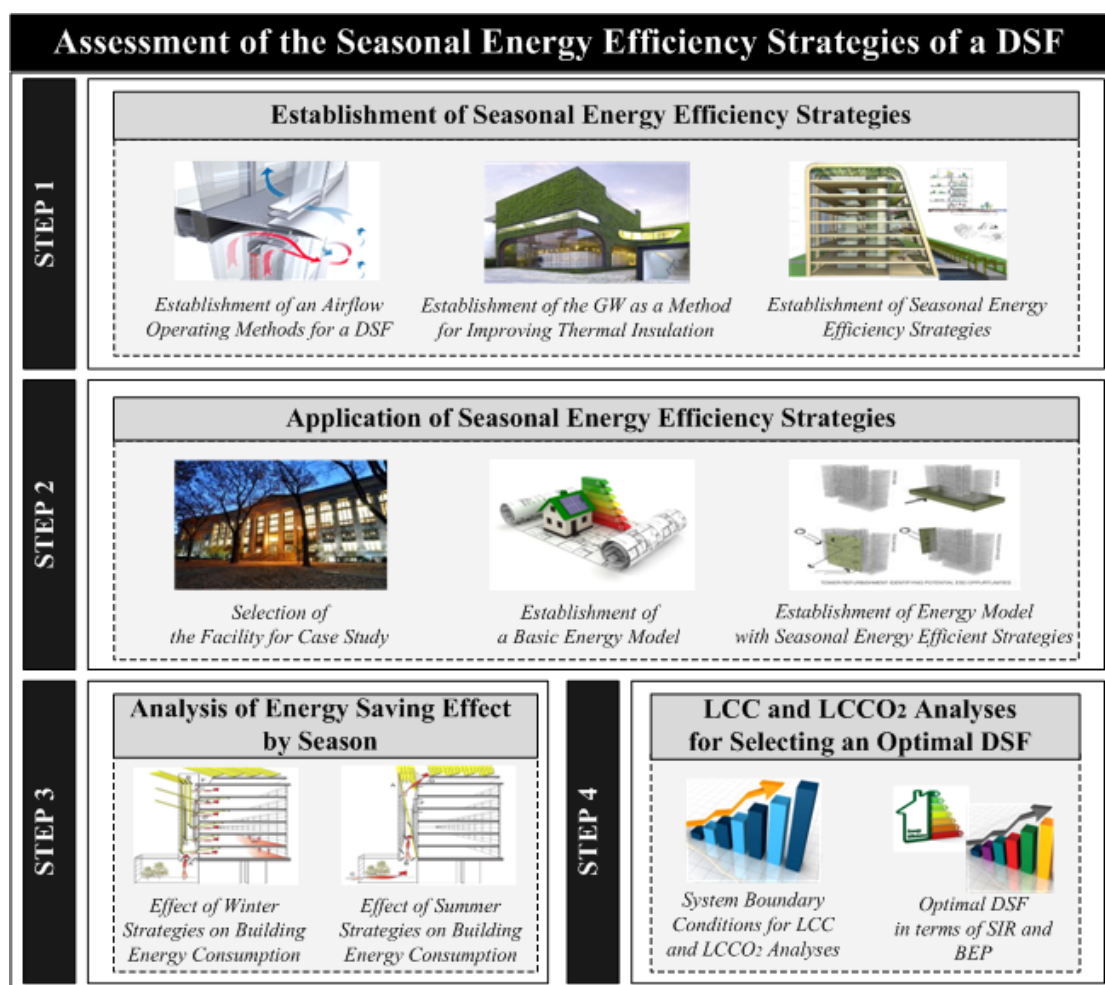
2. Establishment of Seasonal Energy Efficiency Strategies

As mentioned above, this study aimed to establish energy efficiency strategies focus on hot summers and cold winters. Under these seasonal characteristics, the airflow operating methods should be selectively implemented according to hot summers and cold winters. To establish seasonal energy efficiency strategies, this study considered the following methods: (i) a static air buffer as an airflow operating method to improve the effect of DSF in winter; (ii) an external air curtain as an airflow operating method to improve the effect of DSF in the summer; (iii) natural ventilation as an airflow operating method to improve the additional effect of DSF in summer; and (iv) GW as a method for improving thermal insulation to improve the effect of DSF in both summer and winter. Based on these methods, this study established seasonal energy efficiency strategies in summer and in winter.

2.1. Establishment of an Airflow Operating Method for a DSF

To establish the seasonal energy efficiency strategies of a DSF that can reduce the heating and cooling energy consumption, airflow operating methods that consider the climatic environment should be established. DSF can be categorized by the airflow operating methods and shapes. A review of over 60 historical cases of DSFs installed globally shows that the airflow operating methods and shapes of

DSF are variable depending on installation purposes and climatic environments [12,39]. These historical cases presented the operating strategies of a DSF according to the seasonal characteristics rather than those in specific region or climate.

The airflow operating methods of DSF depend on the airflow types of DSF. Meanwhile, the airflow types are variable depending on the types of openings installed in the cavity. As shown in Figure 2, airflow type can be divided into a total of six types, based on the opening and closing of the openings: (i) external air curtain (#1, #2); (ii) internal air curtain (#3, #4); (iii) supply air (#5, #6); (iv) exhaust air (#7, #8); (v) full open (#9); and (vi) static air buffer (#10).

Figure 2. Airflow types of double skin façade.
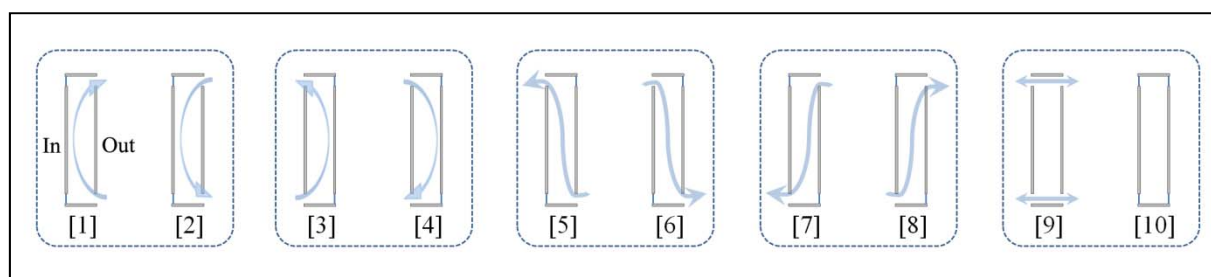
In the East Asian monsoon climates with clear seasonal characteristics, the airflow operating methods should be implemented selectively according to season. In winter, it would be advantageous in terms of thermal comfort to close the openings since external temperature is always lower than inside the building. Existing studies and cases have shown that, as mentioned in the introduction, the static air buffer is the optimal type in winter because it acts as a thermal buffer [9–15,38] (Figure 3a).

Figure 3. Seasonal airflow operating method of a DSF: (**a**) Static air buffer as winter airflow operating method; (**b**) External air curtain as summer airflow operating method; (**c**) Natural ventilation as summer airflow operating method.
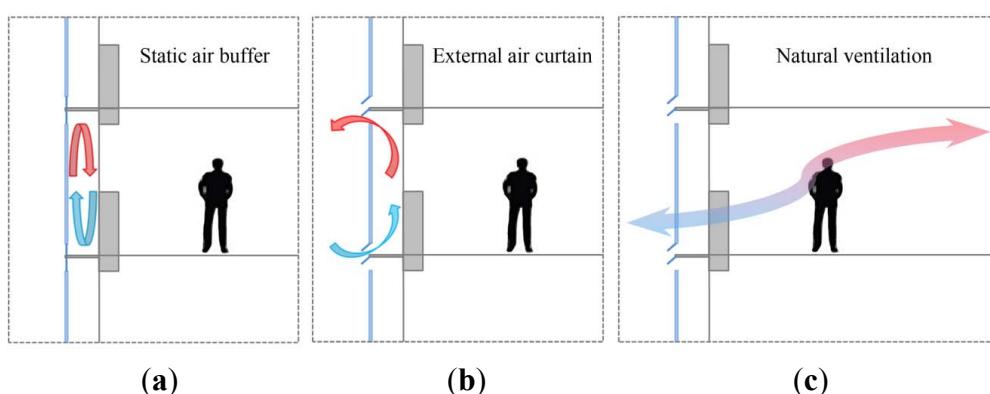

In summer, an airflow operating method should be used appropriately since the relationship among the temperature outside the cavity, inside the cavity, and inside the building changes over time. Within the duration of sunshine, in which the external temperature is higher than inside the building, closing the openings inside the building would be advantageous in terms of thermal comfort since the heat gained by solar radiation would be removed in the cavity before it enters the building. Therefore, as mentioned in the introduction, the external air curtain is the optimal type because it can extract heat

gained by solar radiation [40–42] (Figure 3b). Meanwhile, after sunset, when external temperature becomes lower than inside the building, natural ventilation, in which the openings of the cavity are opened, can emit heat inside the building. Therefore, to save cooling energy consumption, natural ventilation can be used according to specific circumstances [18–20] (Figure 3c).

Therefore, this study used the seasonal airflow operating methods of a DSF in the following situations: (i) the static air buffer is used in winter; (ii) the external air curtain is used in summer; and (iii) supplementally, natural ventilation is used strategically in summer.

Meanwhile, the shape of DSF can be generally divided into four types based on the cavity unit of the space that is divided vertically and horizontally [4,43] (Figure 4): (i) the box type with the cavity unit in each room that is divided vertically and horizontally; (ii) the corridor type with the cavity unit in each floor that is divided horizontally; (iii) the multistory type with a cavity unit on the side of the façade; and (iv) the shaft box type adding the box type to solar chimney.

Figure 4. The shape and airflow of DSF: (**a**) Box type; (**b**) Corridor type; (**c**) Multistory type; (**d**) Shaft box type.

(**a**)   (**b**)

(**c**)   (**d**)
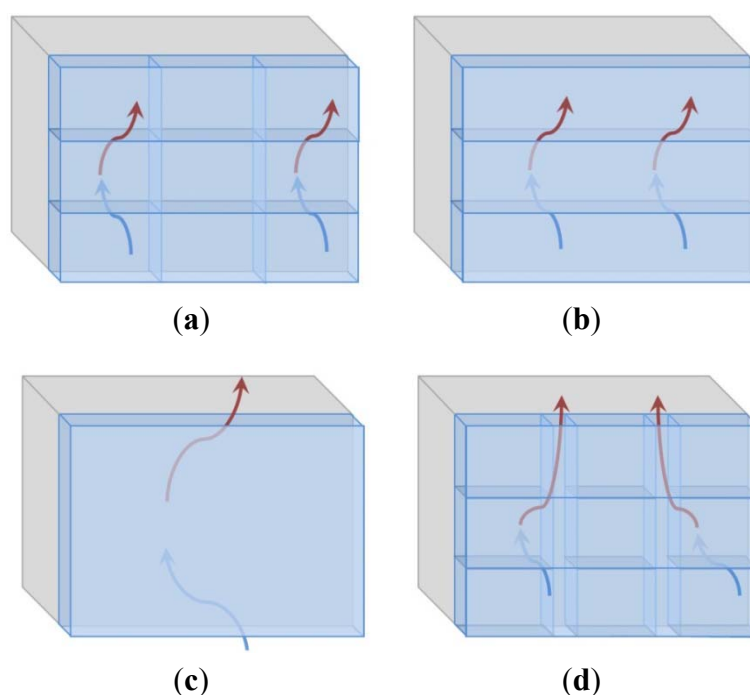
The box type and the shaft type, which have a cavity unit in each room, have been used mostly for sound insulation. The multistory type, which has a cavity unit in the façade, has been used widely to save construction cost since it requires relatively smaller materials and would be advantageous in terms of natural lighting (Table 1). However, the heating and cooling energy saving effects of these four types of DSF are variable depending on seasonal characteristics and there is no clear priority on which type is optimal to use [44]. Therefore, this study conducted a comparative analysis of these four types of DSF in terms of energy-saving effects by implementing the aforementioned airflow operating methods by season.

Table 1. Characteristics of the four types of DSF.

DSF type	Box	Corridor	Multistory	Shaft box
Vertical division	O	X	X	O
Horizontal division	O	O	X	O
Sound insulation	Good	Satisfactory	Satisfactory	Good
Used material	Many	Medium	Less	Very many
Natural lighting	Good	Very good	Very good	Satisfactory

Note: DSF stands for the double skin façade.

2.2. Establishment of the GW as a Method for Improving Thermal Insulation

To establish the seasonal energy efficiency strategies of a DSF that can reduce the heating and cooling energy consumption, this study aimed to select the optimal GW as a method to improve thermal insulation. GWs use mainly three soil types (natural, improved, and artificial soil) and two plant types (sedum and grass). Each type of soil and plant has different characteristics. Therefore, the following criteria were used to select the GW that can offer the highest efficiency in thermal insulation.

First, soil has different characteristics, including thermal insulation, according to type [45,46]. The thickness of soil differs by plant type, which causes differences in thermal insulation [47,48]. Also, the lower the unit load, the easier the soil can be attached to the wall. Therefore, the type of soil was selected by considering thermal insulation and constructability. The thermal insulation of soil is highest in artificial soil, followed by improved and natural soil, while the unit load is in the opposite order [49]. As a result, this study selected artificial soil.

Second, the density of foliage and leaf area index (LAI) differs according to the type of plant. The higher the LAI of the plant, the higher its sunblock properties, resulting in further reduction of the thermal bridge effect [50]. The LAI of grass is 2.5, which is higher than that of sedum (2), thus, offering superior sunblock effect. Furthermore, the thickness of grass soil is 0.15 m, which is thicker than that of sedum (0.1 m), which offers higher thermal insulation. Based on artificial soil, the construction cost of grass is $106.43, which is lower than that of sedum at $133.03 [51,52]. Therefore, this study used artificial soil and grass (refer to Table 2). The selected GW plant, Kamtschaticum, has spread throughout East Asia such as China, Japan, Sakhalin, Kuril, and Amour as well as South Korea. The climate conditions of these regions are similar to those of South Korea [49].

Table 2. Properties of selected green wall.

Soil (artificial)		Plant (grass)	
Conductivity of dry soil (W/m·K)	0.2	Height of plants (m)	0.15
		Thickness of soil (m)	0.15
Specific heat of dry soil (J/kg·K)	800	Leaf area index (dimensionless)	2.5
		Leaf reflectivity (dimensionless)	0.11
Density of dry soil (kg/m^3)	300	Leaf emissivity	0.9
		CO_2 absorption (kgCO$_2$/m^2/year)	5.7

2.3. Establishment of Seasonal Energy Efficiency Strategies

In Sections 2.1 and 2.2, this study selected four applicable methods to establish seasonal energy efficiency strategies. Then, after dividing them into summer and winter, this study established seasonal energy efficiency strategies. First, the following two methods were combined to establish season energy efficiency strategies for winter: (i) static air buffer (Method_A1) as an airflow operating method; and (ii) GW (Method_B) for improving thermal insulation. Next, to establish energy efficiency strategies in summer, the following three methods were combined: (i) external air curtain (Method_A2) as an airflow operating method; (ii) natural ventilation (Method_A3) as an airflow operating method; and (iii) GW (Method_B) as a method to improve thermal insulation (refer to Table 3).

Table 3. Seasonal energy efficiency strategies.

Seasonal energy efficiency strategies	Airflow operating method			Method for improving thermal insulation
	Winter	Summer		Winter and Summer
	(Method_A1) Static air buffer	(Method_A2) External air curtain	(Method_A3) Natural ventilation	(Method_B) Green wall
Winter strategies	O	-	-	-
	O	-	-	O
Summer strategies	-	O	-	-
	-	O	O	-
	-	O	O	O

3. Application of Seasonal Energy Efficiency Strategies

3.1. Selection of the Facility for Case Study

To analyze the applicability of the seasonal energy efficiency strategies for a DSF, it is necessary to select a target facility. To acquire the feasibility of the analysis, the following criteria for selecting a target facility were established:

- The East Asian monsoon climate region with clear summer and winter characteristics was selected as a target region to determine the energy-saving effect of the seasonal energy efficiency strategies for a DSF;
- DSF results in the heat transfer from the temperature difference among the external skin, cavity, and the inner skin of a building. Therefore, this study aimed to determine the performance of DSF itself by analyzing a building whose energy usage pattern is evenly distributed day and night;
- The type of target facility that is statistically significant in terms of energy consumption was selected, resulting in a great effect on the whole energy consumption of South Korea.

Based on the criteria above, this study selected the Y University library facility, which is located in Seoul, South Korea, the East Asian monsoon climate region with clear summer and winter seasons, as the target building. It also has long operational hours. As shown in Table A1, the space configuration of the library facility consists of reading rooms, study rooms, and PC seats. Especially, the study rooms and PC seats open 24 hours all the year round. Furthermore, air-conditioning and heating system are

automatically operated 24 hours a day. It was determined that the energy consumption of the university facilities in 2010 was 295 thousand TOE, which is ranked second among all types of buildings in South Korea [53] (refer to Table A2). Especially, the library facility is the main factor of energy consumption and exists in all the university [54]. Furthermore, the most of the university library opens 24 h a day such as "Y" university library.

3.2. Establishment of a Basic Energy Model

To analyze the effect of the DSF on the target building, a basic energy model that reflects the current energy consumption pattern should be established. Toward this end, this study used a building energy simulation software program called, *DesignBuilder* which was developed in the UK. *DesignBuilder* is a fully featured version of *EnergyPlus*, which was developed by U.S. Department of Energy. It was developed to be available at any stage of the design process.

First released in 2005, *DesignBuilder* allows a wide range of building types to be simulated using the latest version of *EnergyPlus*. Using advanced design options such as natural ventilation, daylight control, DSF, chilled beams, and heated floors, it can evaluate its impact on the building environmental performance, comfort, cost, and daylight availability [55]. It calculates the heating and cooling loads using the ASHRAE-approved 'heat balance' method implemented in *EnergyPlus*. There are some previous research which analyzes the DSF through *EnergyPlus* or *DesignBuilder* [3,56–62]. Building-related characteristics, as well as user-related characteristics, should be considered in conducting building energy simulation [63]. First, building-related characteristics refer to factors related to the energy efficiency of the building, such as the type and size of the building, the material and standard of detailed components, and heating and cooling system. The front entrance of the target building is facing east, and some parts of the first floor are in a Pilotis structure. To reflect such characteristics, architectural drawings and specifications of the target library facility were used.
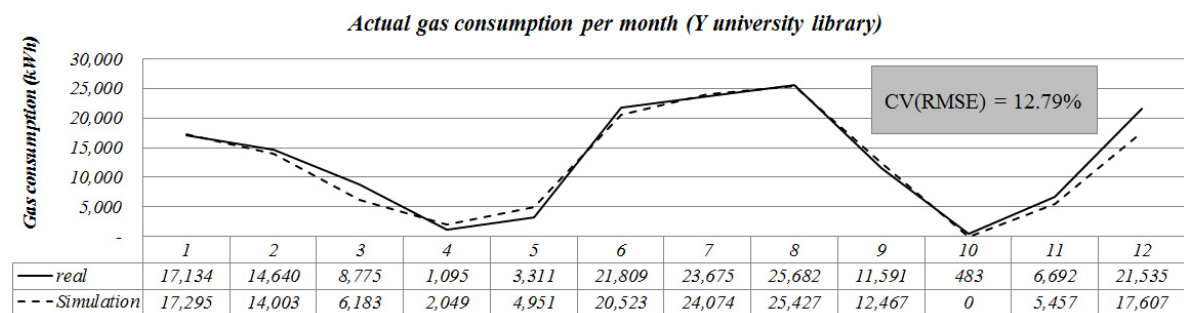
Second, user-related characteristics refer to factors related to the energy efficiency of the building, such as occupancy profile and electronic appliance usage schedules. The average occupancy was 1000 per floor based on the survey of a daily average number of people entering the facility and the number of seats. Data on lighting, computers, and office appliances were based on architectural drawings and a field survey. To reflect these characteristics, this study collected the yearly heating and cooling energy consumption data from the manager in charge of machinery room in the target building (Table 4).

To verify the feasibility of the building energy simulation results, tolerance limits for energy simulation offered by the American Society of Heating, Refrigerating and Air-conditioning Engineers (*i.e.*, the coefficient of variation of the root mean square error (CV(RMSE)) were used [Equation (1)] in the monthly difference between actual energy consumption and the simulation-based energy consumption.
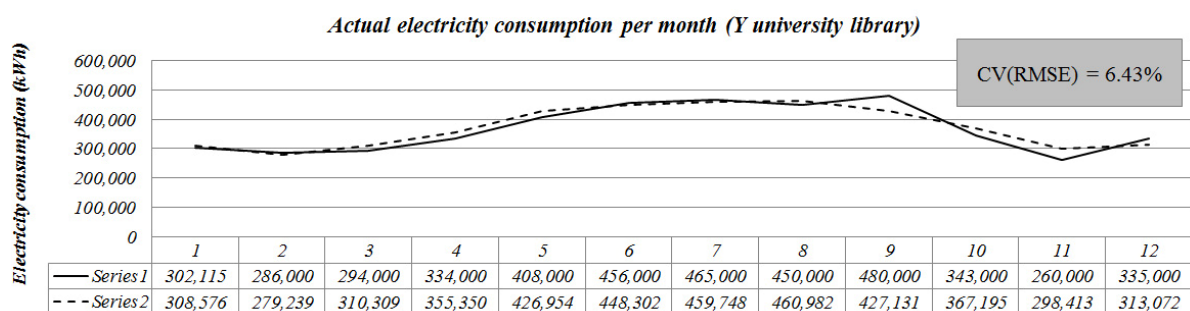
Table 4. Simulation model information of the basic energy model.

Classification	Detailed descriptions	
General information	Weather data	Climate data in Seoul, Korea
	Run period	January 2012–December 2012
	Schedule	Office and library schedule
	Conditioning system	GHP (gas-engine driven heat pump)
	Heating period	January–May, November–December
	Cooling period	March–September
	Shading device	High reflective roller blind
	Total floor area	6 stories, 16,409.17 m^2
	Applicable area for DSF	645.536 m^2
	Applicable area for GW	385.256 m^2
Cooling load	Occupancy	0.3 (people/m^2)
	Lighting	400 lux
	Office equipment	10 (W/m^2)
Global thermal characteristics of each wall (thickness/conductivity)	Ground floor	332.7 (mm)/0.250 (W/m^2 K)
	External floor	178.2 (mm)/0.250 (W/m^2 K)
	Floor	100 (mm)/4.730 (W/m^2 K)
	Roof	367.5 (mm)/0.250 (W/m^2 K)
	Ceiling	100 (mm)/4.730 (W/m^2 K)
	External wall	292.5 (mm)/0.350 (W/m^2 K)
	Internal partition	150 (mm)/1.923 (W/m^2 K)
	External glazing	25 (mm)/2.708 (W/m^2 K)
	Internal glazing	25 (mm)/2.708 (W/m^2 K)

Figure 5. (CV)RMSE: (**a**) Gas consumption ("Y" university library); (**b**) Electricity consumption ("Y" university library).

Actual gas consumption per month (Y university library)

CV(RMSE) = 12.79%

	1	2	3	4	5	6	7	8	9	10	11	12
real	17,134	14,640	8,775	1,095	3,311	21,809	23,675	25,682	11,591	483	6,692	21,535
Simulation	17,295	14,003	6,183	2,049	4,951	20,523	24,074	25,427	12,467	0	5,457	17,607

(**a**)

Actual electricity consumption per month (Y university library)

CV(RMSE) = 6.43%

	1	2	3	4	5	6	7	8	9	10	11	12
Series1	302,115	286,000	294,000	334,000	408,000	456,000	465,000	450,000	480,000	343,000	260,000	335,000
Series2	308,576	279,239	310,309	355,350	426,954	448,302	459,748	460,982	427,131	367,195	298,413	313,072

(**b**)

The CV (RMSE) values were 12.79% (gas energy consumption) and 6.43% (electricity energy consumption) within the tolerance limits (25%) [45] (Figure 5). Thus, it was determined that the basic energy model was feasible:

$$CV(RMSE) = \frac{\sqrt{\sum_{i=1}^{n}(AEC_i - SEC_i)^2 \times \frac{1}{n}}}{\sum_{i=1}^{n}AEC_i \times \frac{1}{n}} \times 100 \tag{1}$$

where *AEC* is the actual energy consumption; *SEC* is the simulation-based energy consumption; and *n* is the number of data (months).

3.3. Establishment of Energy Models with Seasonal Energy Efficiency Strategies

In Chapter 2, this study established seasonal energy efficiency strategies in summer and in winter to improve the effect of DSF implementation (refer to Table 3). Based on these strategies, this study established energy models with seasonal energy efficiency strategies by DSF types, as shown in Table 5.

Table 5. Establishment of energy models with seasonal energy efficiency strategies.

Classification	Energy model	Seasonal energy efficiency strategies	Airflow operating method			Method to improve thermal insulation
			Winter	Summer		All seasons
			(Method_A1) Static air buffer	(Method_A2) External air curtain	(Method_A3) Natural ventilation	(Method_B) Green wall
Existing facility	BEM	-	-	-	-	-
Box type DSF	EM$_B$ #1	Winter strategies	O	-	-	-
	EM$_B$ #2	Winter strategies	O	-	-	O
	EM$_B$ #3	Summer strategies	-	O	-	-
	EM$_B$ #4	Summer strategies	-	O	O	-
	EM$_B$ #5	Summer strategies	-	O	O	O
Corridor type DSF	EM$_C$ #1	Winter strategies	O	-	-	-
	EM$_C$ #2	Winter strategies	O	-	-	O
	EM$_C$ #3	Summer strategies	-	O	-	-
	EM$_C$ #4	Summer strategies	-	O	O	-
	EM$_C$ #5	Summer strategies	-	O	O	O
Multistory type DSF	EM$_M$ #1	Winter strategies	O	-	-	-
	EM$_M$ #2	Winter strategies	O	-	-	O
	EM$_M$ #3	Summer strategies	-	O	-	-
	EM$_M$ #4	Summer strategies	-	O	O	-
	EM$_M$ #5	Summer strategies	-	O	O	O
Shaft box type DSF	EM$_S$ #1	Winter strategies	O	-	-	-
	EM$_S$ #2	Winter strategies	O	-	-	O
	EM$_S$ #3	Summer strategies	-	O	-	-
	EM$_S$ #4	Summer strategies	-	O	O	-
	EM$_S$ #5	Summer strategies	-	O	O	O

Note: BEM stands for the basic energy model, EM$_B$ stands for Box type DSF energy model, EM$_C$ stands for corridor type DSF energy model, EM$_M$ stands for multistory type DSF energy model, and EM$_S$ stands for shaft box type DSF energy model.

4. Analysis of Energy-Saving Effect by Season

The energy analysis of DSF energy models, which implemented seasonal energy efficiency strategies, shows the effect of such strategies. As shown in Table 6, this study proposed the energy consumption of each energy model. For a detailed analysis on the effect of the introduction of the strategies, this study analyzed the first DSF type, the box type.

### 4.1. Effect of Winter Strategies on Building Energy Consumption

As shown in Table 6, winter energy efficiency strategies can be divided into two types: (i) static air buffer (Method_A1) as an airflow operating method; and (ii) GW (Method_B) as a method to improve thermal insulation.

4.1.1. Effect of the Winter Strategy (Method_A1)

In winter, the heating energy-saving effect of EMB #1 with the static air buffer (Method_A1) was 3.20% of the basic energy model, reflecting a decrease in the winter heating energy consumption (Table 6).

There was a substantial temperature gap between the cavity of EM_B #1 and outside the building (line in Figure 6). The temperature of the cavity continued to increase by the hour due to the heat gained by solar radiation within the duration of sunshine, showing a notable difference of up to 35.77 °C at 1:30 pm (EM_B #1: 30.27 °C; outside: −4.5 °C). Even when the heat generator is not operational, the temperature difference outside and inside the building was still over 15 °C. Thus, the heat inside the building was kept from being emitted outside, and EM_B #1 consumed lesser heating energy than the basic energy model (bar graphs in Figure 6). In winter, the airflow operating method in EM_B #1 was found to maintain the temperature inside the building and inside the cavity to a maximum.

Figure 6. Temperature-time profile and heating energy consumption on a winter day (basic energy model *vs.* EM_B #1).
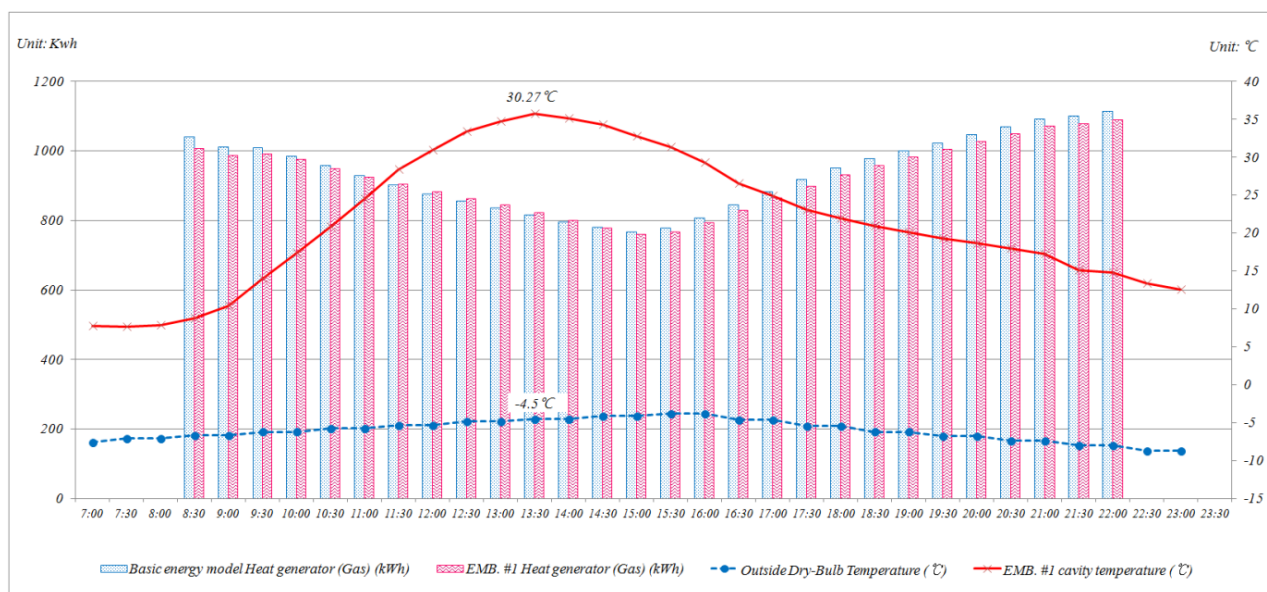
Table 6. Gas consumption by energy models with seasonal energy efficiency strategies.

| Classification	Energy model	Seasonal energy efficiency strategies		Energy consumption			
				Winter		Summer	
				Consumption (kWh)	Saving rate (%)	Consumption (kWh)	Saving rate (%)
Existing facility	BEM	-		671,142	-	993,745	-
Box type DSF	EM_B #1	Winter	(Method_A1)	649,678	3.20	-	-
	EM_B #2		(Method_A1 + B)	648,541	3.37	-	-
	EM_B #3	Summer	(Method_A2)	-	-	1,008,888	−1.52
	EM_B #4		(Method_A2 + A3)	-	-	881,119	11.33
	EM_B #5		(Method_A2 + A3 + B)	-	-	880,261	11.42
Corridor type DSF	EM_C #1	Winter	(Method_A1)	657,496	2.03	-	-
	EM_C #2		(Method_A1 + B)	654,383	2.50	-	-
	EM_C #3	Summer	(Method_A2)	-	-	1,006,296	−1.26
	EM_C #4		(Method_A2 + A3)	-	-	869,348	12.52
	EM_C #5		(Method_A2 + A3 + B)	-	-	868,851	12.57
Multistory type DSF	EM_M #1	Winter	(Method_A1)	655,313	2.36	-	-
	EM_M #2		(Method_A1 + B)	652,217	2.82	-	-
	EM_M #3	Summer	(Method_A2)	-	-	1,003,995	−1.03
	EM_M #4		(Method_A2 + A3)	-	-	868,302	12.62
	EM_M #5		(Method_A2 + A3 + B)	-	-	867,844	12.67
Shaft box type DSF	EM_S #1	Winter	(Method_A1)	644,507	3.97	-	-
	EM_S #2		(Method_A1 + B)	643,399	4.13	-	-
	EM_S #3	Summer	(Method_A2)	-	-	1,020,428	−2.69
	EM_S #4		(Method_A2 + A3)	-	-	903,837	9.05
	EM_S #5		(Method_A2 + A3 + B)	-	-	870,575	12.39

Note: BEM stands for the basic energy model, EM_B stands for Box type DSF energy mode; EM_C stands for corridor type DSF energy model; EM_M stands for multistory type DSF energy model; EM_S stands for the shaft box type DSF energy model; Method_A1 stands for static air buffer; Method_B stands for green wall; Method_A2 stands for external air curtain; Method_A3_stands for natural ventilation.

4.1.2. Effect of Winter Strategies [(Method_A1) and (Method_B)]

In winter, the heating energy saving effect of EM_B #2, which used the static air buffer (Method_A1) and green wall (Method_B), was 3.37% larger than EM_B #1 (3.20%), which used only the static air buffer (Method_A1) (Table 6). For a more detailed analysis, this study focused on the data on December 5, when the temperature was one of the lowest recorded for the year. Compared to the temperature inside the cavity, EM_B #2 was lower than EM_B #1, meaning that the amount of heat emitted from inside the building to the cavity was small (lines in Figure 7). GW blocked the heat transfer by improving the thermal insulation of the wall. As a result, EM_B #2 (648,541 kWh) had lesser heating energy consumption than EM_B #1 (649,678 kWh) (Table 6). In conclusion, the thermal bridge effect due to the improvement in thermal insulation was reduced by applying GW to the inner skin wall of DSF, resulting in heating energy savings effect in winter.

Based on the result above, two strategies were found effective in saving heating energy consumption: (i) preserving heat in the cavity through the static air buffer in winter (Method_A1) (EM_B #1 compared with the basic energy model); and (ii) reducing the heat emitted from inside the building by reducing the thermal bridge effect with GW in winter (Method_B) (EM_B #2 compared with EM_B #1).

Figure 7. Temperature-time profile and heating energy consumption on a winter's day (EM_B #2 *vs.* EM_B #1).
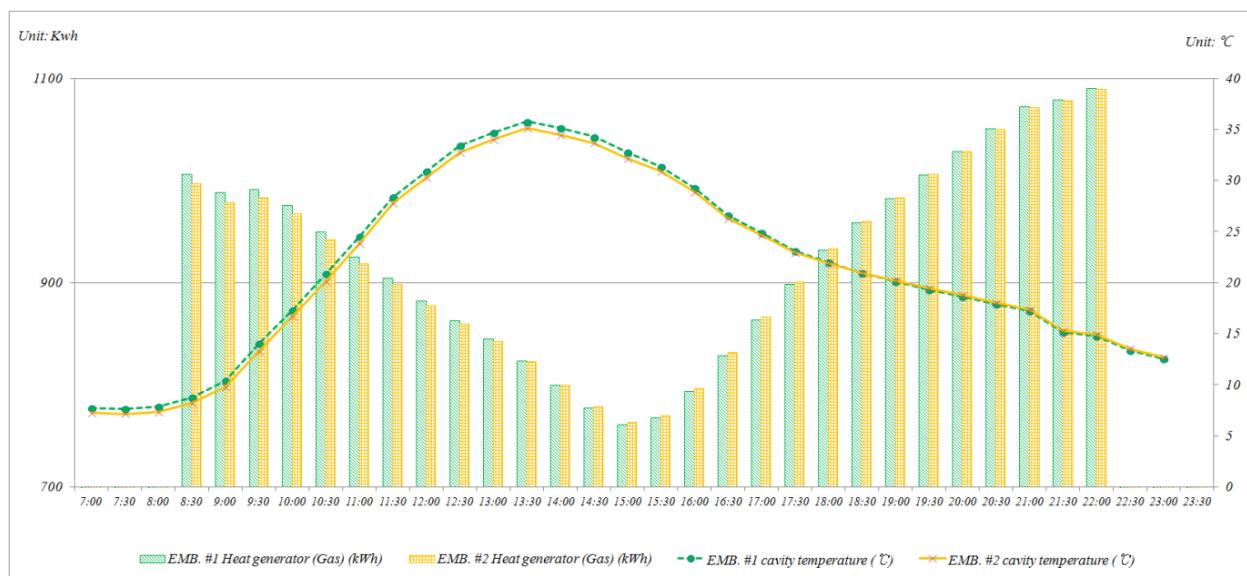
4.2. Effect of Summer Strategies on Building Energy Consumption
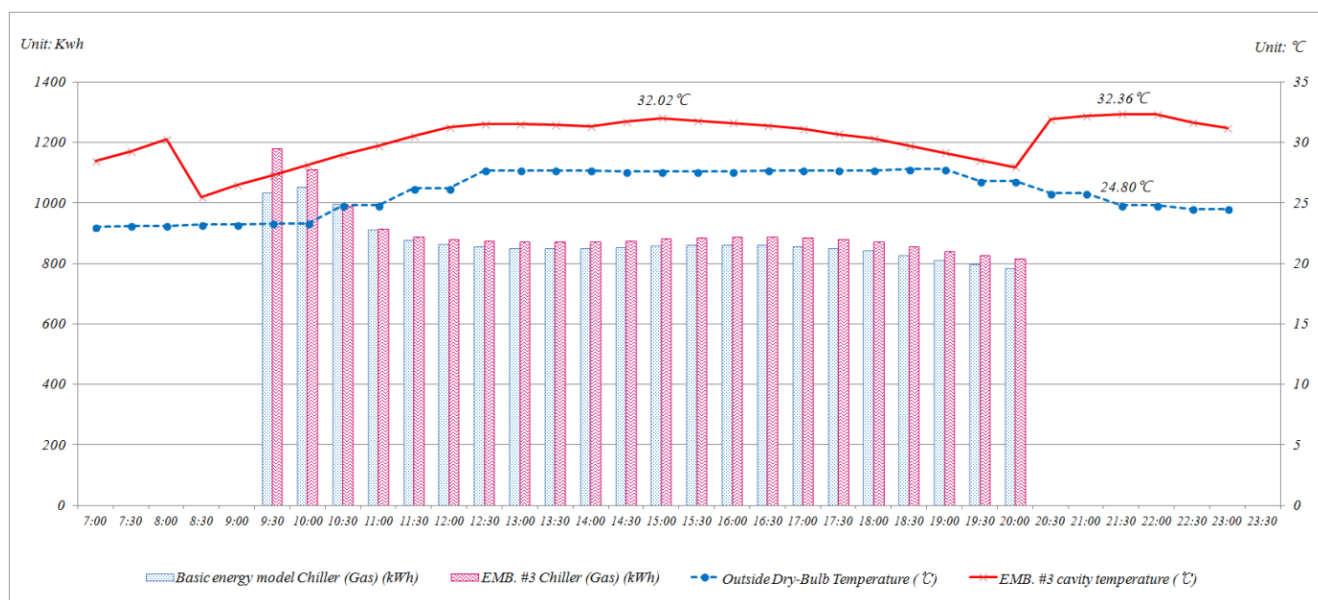
4.2.1. Effect of Summer Strategy (Method_A2)

As shown in Table 6, summer energy efficiency strategies can be divided into three parts: (i) external air curtain (Method_A2) as an airflow operating method; (ii) natural ventilation (Method_A3) as an airflow operating method; and (iii) GW (Method_B) as a method to improve thermal insulation.

In summer, the cooling energy saving effect of EM_B #3, which used the external air curtain (Method_A2) as an airflow operating method, was −1.52% (Table 6). Namely, the summer cooling energy consumption increased. For a more detailed analysis, this study focused on the data on 3 August,

when the temperature was one of the highest for the year. There was a significant temperature gap between the cavity of EM$_B$ #3 and outside the building (lines in Figure 8). The temperature of the cavity did not go over 32.02 °C (at 15:00) during the duration of sunshine due to the external air curtain (Method_A2). However, after the duration of sunshine (from 20:00 to 9:30), the chiller was turned off, so the temperature inside the building rose. At this time, the maximum temperature difference between the cavity and inside the building was 7.56 °C at 21:30 (EM$_B$ #3: 32.36 °C; outside: 24.80 °C), which was maintained almost throughout. Heat was not emitted outside the building, and to reduce the temperature inside the building, higher cooling energy consumption would be required than that of the basic energy model (bar graphs in Figure 8). Therefore, additional methods are required for the external air curtain (Method_A2) of EM$_B$ #3 during summer to reduce the temperature inside the building and in the cavity after the duration of sunshine.

**Figure 8.** Temperature-time profile and cooling energy consumption on a summer day (basic energy model *vs.* EM$_B$ #3).

4.2.2. Effect of Summer Strategies [(Method_A2) and (Method_A3)]

As shown in Table 6, the cooling energy saving effect of EM$_B$ #4, which added natural ventilation (Method_A3) to EM$_B$ #3, was 11.33%. Compared to EM$_B$ #3 (−1.52%), where cooling energy consumption increased in summer, EM$_B$ #4 shows considerable amount of energy saving. For a more detailed analysis, this study focused on the data on 3 August, when the temperature was one of the highest for the year.

Furthermore, there was a significant temperature gap between the cavity of EM$_B$ #4 and EM$_B$ #3 from 20:00 to 9:30 (dotted lines in Figure 9). First, during the duration of sunshine prior to the operation of the chiller, the cavity temperature of EM$_B$ #4 was lower than that of EM$_B$ #3 by up to 6.59 °C at 8:00 (EM$_B$ #4: 23.65 °C; EM$_B$ #3: 30.24 °C). Also, the temperature inside the building in EM$_B$ #4 was lower by up to 8.45 °C compared to that of EM$_B$ #3 (EM$_B$ #4: 26.07 °C; EM$_B$ #3: 34.52 °C) (solid lines in Figure 9). Namely, EM$_B$ #4, which added natural ventilation (Method_A3) when the chiller was not operational, prevented the rise in temperature due to solar radiation. Second, after the

chiller ceased operating (from 21:00), natural ventilation (Method_A3) continued to reduce the temperature inside the building and in the cavity. Due to the lowered temperature inside the building, EM_B #4 consumed lesser cooling energy than EM_B #3 (bar graphs in Figure 9). In conclusion, the cooling energy saving effect was achieved by establishing summer airflow operating methods, including natural ventilation (Method_A3).

Figure 9. Temperature-time profile and cooling energy consumption on a summer day (EM_B #4 *vs.* EM_B #3).
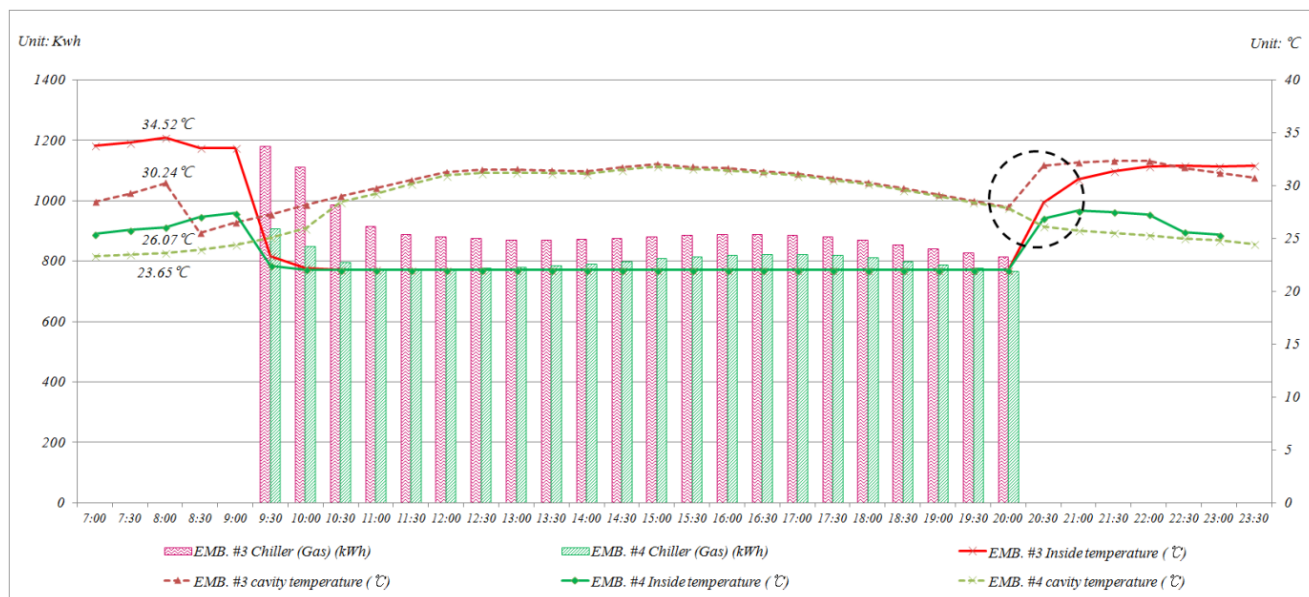
4.2.3. Effect of Summer Strategies [(Method_A2), (Method_A3) and (Method_B)]

Another strategy in reducing the inflow of heated air in the cavity to inside the building is by cutting down the thermal bridge effect by increasing the thermal insulation of the inner skin. The heat from the cavity to inside the building in summer can be reduced by using GW. In summer, the cooling energy saving effect of EM_B #5 was 11.42%, which was more than that of EM_B #4 (11.32%) (Table 6). For a more detailed analysis, this study focused on the data on 3 August, when one of the highest temperatures for the year was recorded. The cavity temperature of EM_B #5 was higher than that of EM_B #4, meaning the inflow of heated air from the cavity to inside the building was smaller (Figure 10). Namely, GW reduced the thermal bridge effect and prevented heat transfer. As a result, the cooling energy consumption in EM_B #5 (880,261 kWh) was reduced, compared to EM_B #4 (881,119 kWh).

A similar tendency in energy savings attributed to the implementation of seasonal energy efficiency strategies was observed in corridor DSF, multistory DSF, and shaft box DSF (refer to Table 6). EM_C #1 (2.03%), EM_M #1 (2.36%), and EM_S #1 (3.97%), which used the static air buffer (Method_A1), showed higher heating energy savings compared to the existing facility. Additionally, EM_C #2 (2.50%), EM_M #2 (2.82%), and EM_S #2 (4.13%), which used GW (Method_B) to improve thermal insulation, showed higher heating energy savings than the EM_C #1, EM_M #1, and EM_S #1.

EM_C #4 (12.52%), EM_M #4 (12.62%), and EM_S #4 (9.05%), which used both external air curtain (Method_A2) and natural ventilation (Method_A3), showed higher cooling energy savings than the existing facility. Furthermore, EM_C #5 (12.57%), EM_M #5 (12.67%), and EM_S #5 (12.39%), which

used GW (Method_B) to improve thermal insulation, showed larger cooling energy savings than the EM$_C$ #4, EM$_M$ #4, and EM$_S$ #4. Based on the results above, the seasonal energy efficiency strategies for saving heating and cooling energy consumption were effective.

Figure 10. Temperature-time profile and cooling energy consumption on a summer day (EMB #4 *vs.* EMB #5).
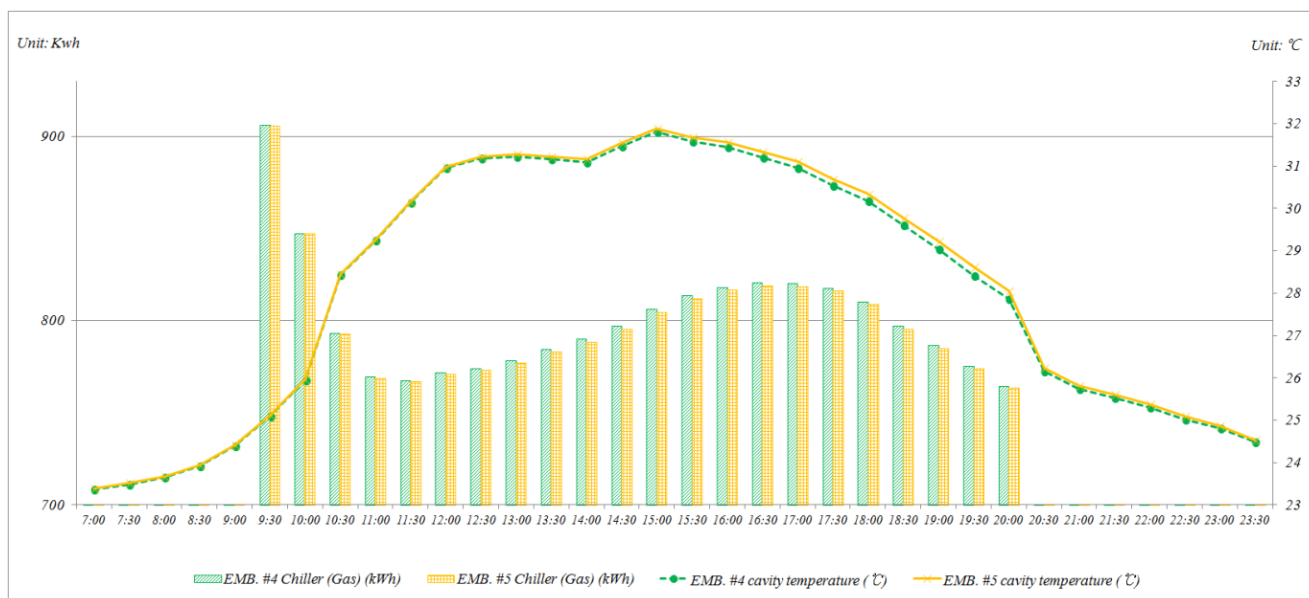
5. LCC and LCCO$_2$ Analyses for Selecting an Optimal DSF

5.1. System Boundary Conditions for LCC and LCCO$_2$ Analyses

By analyzing the energy-saving effects of the aforementioned energy models, an optimal DSF type in terms of energy savings can be selected. However, considering the constraints of the limited budget, a DSF type with the highest return on investment should be chosen. Therefore, this study conducted an economic and environmental assessment from the life cycle perspective. It considered reducing CO_2 emission by saving energy consumption for the environmental assessment [Equation (2)]. The quantity of CO_2 emission from heating and cooling energy consumption was converted into an economic value based on the profit from the sale of carbon credits, which is referred to as "Korea Certified Emission Reduction (KCERs)," ($10.46/tCO_2$ equiv.) [64,65].

$$
\begin{aligned}
&\textit{The amount of } CO_2 \textit{ emission from gas energy consumption } (tCO_2) = \\
&\left(\textit{The yearly amount of gas energy consumption } (m^3)\right) \times \\
&\left(\textit{The ratio of the carbon emission factor of gas energy } \left(\frac{tC}{m^3}\right)\right) \times \\
&\left(\textit{The ratio of the molecular weight of } CO_2 \textit{ to carbon } \left(\frac{tCO_2}{tC}\right)\right)
\end{aligned}
\tag{2}
$$

where the ratio of the carbon emission factor of gas energy is 0.0006083 tC/m^3, and the ratio of the molecular weight of CO_2 to carbon is 44 tCO$_2$/12 tC.

LCC and LCCO$_2$ analyses should consider six factors: (i) the analysis approach; (ii) a realistic discount rate; (iii) the inflation and increase rate; (iv) the analysis period; (v) the starting point of the analysis; and (vi) the significant cost of ownership [49,66]. Table 7 shows the six factors of LCC and LCCO$_2$ analyses used in this study.

Table 7. Key elements of the LCC and LCCO$_2$ analyses.

Classification		Detailed description
Analysis approach		Present worth method (SIR$_{40}$)
Real discount rate	Interest	3.30%
	Gas	0.11%
	KCERs	2.66%
Analysis period		40 years
Starting point of analysis		2012
Significant cost of ownership	Initial construction cost	Initial investment cost
	Operation & maintenance cost	Replacement/repair cost
		Energy consumption cost
	Operation & maintenance benefit	Gas savings
		Benefit from KCERs

In implementing DSF, a higher savings to investment ratio (SIR) should be selected due to the limited budget. In life cycle perspectives, SIR refers to the ratio of the savings with additional benefit to investment cost that is converted to the present worth [Equation (3)], which is the index for relative evaluation. If SIR ≥ 1, the project is feasible, and its breakeven point (BEP) is achieved. The real interest rate was calculated by the nominal interest rate and the inflation rate [Equation (4)] [67–69].

$$SIR = \frac{\sum_{t=0}^{n} \dfrac{S_t + B_t}{(1+r)^t}}{\sum_{t=0}^{n} \dfrac{I_t}{(1+r)^t}}$$

(3)

where *SIR* is savings to investment ratio; S_t is gas energy savings in year *t*; B_t is benefit from KCERs in year *t*; I_t is investment in year *t*; *r* is the real discount rate; and *n* is the period of the life cycle analysis:

$$i = \frac{(1+i_n)}{(1+f)} - 1$$

(4)

where *i* is the real discount rate; i_n is the nominal interest rate; and *f* is the inflation rate, the gas price growth rate, and the carbon dioxide emission trading price growth rate. The service life of a steel reinforced concrete building was set to 40 years, which was provided by "the Standard Service Life and Service Life Scope Chart in the Enforcement Regulations on Corporate Income Tax Act" [49].

5.2. Optimal DSF in Terms of SIR and BEP

Table 8 shows the results of the LCC and LCCO$_2$ analyses of four DSFs with seasonal energy efficiency strategies. This study analyzed SIR$_{40}$ and BEP from life-cycle perspectives. The results of

the LCC and LCCO$_2$ analyses on each of the DSF are as follows: from the perspective of SIR$_{40}$, the multistory, shaft box, corridor, and box types were analyzed in the order of No. 1 (3.20), No. 2 (3.11), No. 3 (3.05), and No. 4 (2.85), respectively. From the perspective of the BEP, the multistory, shaft box, and box types all took nine years, while the corridor type took 11 years. In summary, the multistory type was selected as an optimal DSF in terms of economic and environmental aspects, because while the investment cost (additional initial cost: $190,743; additional replacement cost: $113,395) was lesser than the others, it achieved higher savings with benefit (life cycle energy saving benefit: $958,399; KCER income: $15,748). The larger the unit of the cavity was, the higher the temperature difference between an opening became, resulting in better ventilation. Thus, more heat emitted from the cavity outside the building translates to higher cooling energy savings.

Table 8. LCC and LCCO$_2$ analyses on four DSF with seasonal energy efficiency strategies.

Double Skin Façade	Additional initial cost	Additional replacement cost	LCES benefit	KCER income	SIR$_{40}$		BEP	
	($)	($)	($)	($)	Value	Rank	Year	Rank
Box type	200,414	120,958	900,559	14,798	2.85	4	9	1
Corridor	195,599	117,192	937,402	15,403	3.05	3	11	4
Multistory	190,743	113,395	958,399	15,748	3.20	1	9	1
Shaft box	203,286	123,204	998,674	16,410	3.11	2	9	1

Note: LCES stands for life cycle energy saving; KCER stands for Korea Certified Emission Reduction; SIR stands for saving to investment ratio; BEP stands for break-even point; and the exchange rate (KRW/USD) is 1,112.5 won to a U.S. dollar (as of May.14.2013).

6. Conclusions

To improve the effect of the DSF implementation, this study established seasonal energy efficiency strategies and analyzed the effect of these strategies through a case study. It aimed to select an optimal DSF in terms of SIR. The university facilities were statistically significant in terms of energy consumption. It was determined that the energy consumption of the university facilities in 2010 was 295 thousand TOE, which is ranked second among all types of buildings in South Korea (refer to Table A2). Especially, the library facility is the main factor of energy consumption and exists in all the university. Therefore, the university library facility could have a great effect on the whole energy consumption of South Korea.

The seasonal energy efficiency strategies were established in summer and in winter. First, to establish winter-energy-efficient strategies, a combination of two methods was considered: (i) static air buffer (Method_A1) as an airflow operating method; and (ii) GW (Method_B) for improving thermal insulation. Next, to establish summer-energy-efficient strategies, a combination of the following three methods was considered: (i) external air curtain (Method_A2) as an airflow operating method; (ii) natural ventilation (Method_A3) as an airflow operating method; and (iii) GW (Method_B) for improving thermal insulation (refer to Table 3).

The energy consumption analysis on the energy models showed that the seasonal energy efficiency strategies were effective during both summer and winter seasons. First, in terms of winter-energy-efficiency strategies, the implementation of the static air buffer (Method_A1) as an

airflow operating method to EM_S #1 (shaft box DSF) resulted in 644,507 kWh, with a reduction rate of up to 3.97% in heating energy consumption. Also, to reduce the thermal bridge effect, the use of GW as a method for improving thermal insulation showed that EM_S #3 (shaft box DSF and GW) was 643,399 kWh with a reduction ratio of up to 4.13% in heating energy consumption.

Next, in terms of summer-energy-efficiency strategies, the implementation of the airflow operating methods including natural ventilation showed that the cooling energy consumption of EM_S #4 (multistory DSF) was 868,302 kWh, with a reduction rate of up to 12.62%. Also, to reduce the thermal bridge effect, the use of GW as a method for improving thermal insulation showed that the cooling energy consumption of EM_S #5 (multistory DSF and GW) was 867,844 kWh with a reduction rate of up to 12.67%.

Finally, to maximize SIR_{40} and minimize BEP_{40} through the LCC and $LCCO_2$ analyses, this study selected an optimal DSF with seasonal energy efficiency strategies, which was the multistory DSF with SIR_{40} (3.20) and BEP_{40} (nine years). The analysis showed that this optimal DSF resulted in smaller investment cost (additional initial cost: $190,743; additional replacement cost: $113,395) and higher savings with benefits (LCES benefit: $958,399; KCER income: $15,748).

The results of this study can be used in making decisions regarding: (i) seasonal energy efficiency strategies to save heating and cooling energy consumption in the East Asian monsoon climate region with a high temperature gap in summer and in winter; and (ii) application not only to existing buildings but also for new buildings.

The research team plans to conduct the following future research: (i) an optimal design according to the types of DSFs in terms of energy performance based on cavity depth, the size of an opening, and the position of the shading device of a DSF; (ii) airflow operating methods by season as well as optimal airflow operating methods that change in real-time, depending on the change in temperature inside and outside the building; (iii) thermal bridge effect reduction through thermal insulation of the applied GW, as well as the effects of sunblock and air purification of the applied GW; and (iv) decision support system for the sustainable design and management of buildings based on the long term validation with consideration of the deterioration process.

Conflicts of Interest

The authors declare no conflict of interest.

Appendix

Table A1. Space configuration and operating hours of target library ("Y" university library).

Space configuration	Floor	Operating hours
Reading rooms	2–5 Floor	AM 6–PM 11
Study rooms	1 Floor	Open 24 hours
	6 Floor	Open 24 hours
PC Seats	B1 Floor	Open 24 hours
	6 Floor	Open 24 hours

Table A2. Energy consumption by the types of buildings in South Korea.

Year	2008			2009			2010		
Category	TOE (thousand)	Rate	Rank	TOE (thousand)	Rate	Rank	TOE (thousand)	Rate	Rank
Residential building	487	23.70%	1	453	22.20%	1	462	21.30%	1
University	263	12.80%	3	269	13.20%	2	295	13.60%	2
Department store	267	13.00%	2	260	12.80%	3	292	13.50%	3
Hospital	230	11.20%	4	239	11.70%	4	254	11.70%	4
Hotel	210	10.20%	5	213	10.50%	5	234	10.80%	5
Research Lab	88	4.30%	6	94	4.60%	6	111	5.10%	6
Public building	69	3.40%	7	72	3.50%	7	106	4.90%	7
Telephone company	44	2.10%	8	39	1.90%	8	46	2.10%	8
Non classified	401	19.50%	-	398	19.50%	-	370	17.10%	-
Total	2059	100%	-	2037	100%	-	2170	100%	-

References

1. Heffernan, V. Roofs and the environment; *Can. Consult. Eng.* **2003**, *44*, 35–39.
2. Chicago Climate Exchange. CO$_2$ Market Data 2011. Available online: http://www.chicagoclimatex.com/ market/data/summary.jsf (accessed on 30 May 2013).
3. Chan, A.L.S.; Chow, T.T.; Fong, K.F.; Lin, Z. Investigation on energy performance of double skin façade in Hong Kong. *Energy Build.* **2009**, *41*, 1135–1142.
4. Wang, P.C. Natural Ventilation in Double-Skin Façade Design for Office Buildings in Hot and Humid Climate. Ph.D. Thesis, University of New South Wales, Kensington, Australia, December 2008.
5. Bouden, C. Influence of glass curtain walls on the building thermal energy consumption under Tunisian climatic conditions: The case of administrative buildings. *Renew. Energy* **2007**, *32*, 141–156.
6. Shameri, M.A.; Alghoul, M.A.; Sopian, K.; Zain, M.F.M.; Elayeb, O. Perspectives of double skin façade systems in buildings and energy saving. *Renew. Sustain. Energy Rev.* **2011**, *15*, 1468–1475.
7. Gratia, E.; Herde, A.D. Are energy consumptions decreased with the addition of a double-skin? *Energy Build.* **2007**, *39*, 605–619.
8. Ballestini, G.; Carli, M.D.; Masiero, N.; Tombola, G. Possibilities and limitations of natural ventilation in restored industrial archaeology buildings with a double-skin facade in Mediterranean climates. *Build. Environ.* **2005,** *40*, 983–995.

9. Su, S.; Chen, J. Analysis of heat conduction of anisotropic building materials. *Adv. Mater. Res.* **2011**, *287*, 1227–1232.

10. Stec, W.; Passen, D. Defining the Performance of the Double Skin Facade with the Use of the Simulation Model. In Proceedings of Building Simulation, the 8th International Building Performance Simulation Association (IBPSA) Conference, Eindhoven, The Netherlands, 11–14 August 2003.

11. Pekdemir, E.A.; Muehleisen, R.T. A Parametric Study of the Thermal Performance of Double Skin Facades at Different Climates Using Annual Energy Simulation. In Proceedings of 5th National Conference of International Building Performance Simulation Association IBPSA-USA, Madison, WI, USA, 1–3 August 2012.

12. Rawn, W. *Case Study*: *A Double-Skin Glass Wall*; Associates Architects Inc.: Boston, MA, USA, 2010.

13. Boake, T.M.; Harrison, K.; Chatham, A. *The Tectonics of the Double Skin*: *North American Case Studies*; University of Waterloo: Waterloo, Canada, 2001.

14. Xu, L.; Ojima, T. Field experiments on natural energy utilization in a residential house with a double skin façade system. *Build. Environ.* **2007**, *42*, 2014–2023.

15. Gracia, A.; Navarro, L.; Castell, A.; Pardo, A.R.; Alvarez, S. Experimental study of a ventilated façade with PCM during winter period. *Energy Build.* **2012**, *58*, 324–332.

16. Fukuyo, K. Heat flow visualization for thermal bridge problems. *Int. J. Refrig.* **2003**, *26*, 614–617.

17. Ding, W.; Hasemi, Y.; Yamada, T. Natural ventilation performance of a double-skin facade with a solar chimney. *Energy Build.* **2005**, *37*, 411–418.

18. Mingotti, N.; Chenvidyakarn, T.; Woods, A.W. The fluid mechanics of the natural ventilation of a narrow-cavity double-skin façade. *Build. Environ.* **2011**, *46*, 807–823.

19. Gratia, E.; Herde, A.D. Is day natural ventilation still possible in office buildings with a double-skin façade? *Build. Environ.* **2004**, *39*, 399–409.

20. Gratia, E.; Herde, A.D. Double-skin façade to apartment housing ventilation in an office building with a double-skin façade. *Sol. Energy* **2007**, *81*, 435–448.

21. American Society of Heating, Refrigerating and Air-Conditioning Engineers (ASHRAE). *ASHRAE Guideline 14–2002*; ASHRAE: Atlanta, GA, USA, 2002.

22. Yoshikane, T.; Kimura, F.; Emori, S. Numerical study on Baiu front genesis by heating constrast between land and ocean. *J. Meteorol. Soc. Jpn.* **2001**, *79*, 671–686.

23. Lee, H.W.; Kim, E.J.; Park, S.S.; Choi, J.H. Effects of climate change on the thermal structure of lakes in the Asian Monsoon Area. *Clim. Change* **2012**, *112*, 859–880.

24. Boo, K.O.; Martin, G.; Sellar, A.; Senior, C.; Byun, Y.H. Evaluating the East Asian monsoon simulation in climate models. *J. Geophys. Res. Atmos.* **2011**, *116*, doi: 10.1029/2010JD014737.

25. Webster, P.J.; Magana, V.O.; Palmer, T.N.; Shukla, J.; Tomas, R.A.; Yanai, M.; Yasunari, T. Monsoon: Processes, predictability, and the prospects for prediction. *J. Geophys. Res. Oceans* **1998**, *103*, 14451–14510.

26. Manz, H. Total solar energy transmittance of glass double façades with free convection. *Energy Build.* **2004**, *36*, 127–36.

27. Grande, I.P.; Meseguer, J.; Alonso, G. Influence of glass properties on the performance of double-glazed facades. *Appl. Therm. Eng.* **2005**, *25*, 3163–75.

28. Zhang, X.; Liu, J.; Chen, Z.; Wang, X.; Wang, M.; Ning, L. Thermal bridges in building envelope in hot summer and cold winter areas of thinking. *Appl. Mech. Mater.* **2012**, *117*, 1211–1214.

29. Capozzoli, A.; Gorrino, A.; Corrado, V. A building thermal bridges sensitivity analysis. *Appl. Energy* **2013**, *107*, 229–243.

30. Feist, W.; Peper, S.; Gorg, M. CEPHEUS Project Information No.38: Final Public Report. Available online: http://www.passivehouse.com/ (accessed on 12 August 2013).

31. Evola, G.; Margani, G.; Marletta, L. Energy and cost evaluation of thermal bridge correction in Mediterranean climate. *Energy Build.* **2011**, *43*, 2385–2393.

32. Perez, G.; Rincon, L.; Vila, A.; Gonzalez, J.M.; Cabeza, L.F. Green vertical systems for buildings as passive systems for energy savings. *Appl. Energy* **2011**, *88*, 4854–4859.

33. Di, H.; Wang, D. Cooling effect of ivy on a wall. *Exp. Heat Transf.* **1999**, *12*, 235–45.

34. Akbari, H.; Kurn, D.M.; Bretz, S.E.; Hanford, J.W. Peak power and cooling energy savings of shade trees. *Energy Build.* **1997**, *25*, 139–48.

35. Eumorfopoulou, E.A.; Kontoleon, K.J. Experimental approach to the contribution of plant-covered walls to the thermal behaviour of building envelopes. *Build. Environ.* **2009**, *44*, 1024–1038.

36. Kontoleon, K.J.; Eumorfopoulou, E.A. The effect of the orientation and proportion of a plant-covered wall layer on the thermal performance of a building zone. *Build. Environ.* **2010**, *45*, 1287–1303.

37. Hoyano, A. Climatological uses of plants for solar control and the effects on the thermal environment of a building. *Energy Build.* **1988**, *11*, 181–199.

38. Baldinelli, G. Double skin facades for warm climate regions: Analysis of a solution with an integrated movable shading system. *Build. Environ.* **2009**, *44*, 1107–1118.

39. Kim, S.Y.; Song, K.D. Determining photosensor conditions of a daylight dimming control system using different double-skin envelope configurations. *Indoor Built Environ.* **2007**, *46*, 411–425.

40. Gratia, E.; Herde, A.D.; Natural cooling strategies efficiency in an office building with a double-skin façade. *Energy Build.* **2004**, *36*, 1139–1152.

41. Aleksandar, S.A.; Tanja, B.C.; Damir, D.D.; Ivan, H.S. Development of simple calculation model for energy performance of double skin facades. *Therm. Sci.* **2012**, *16*, S251–S267.

42. Szokolay, S.V. *Introduction to Architectural Science: The Basis of Sustainable Design*, 2nd ed.; Elsevier Science & Technology Books: Burlington, MA, USA, 2008.

43. Poirazis, H. *Double Skin Facades for Office Buildings*; Report EBD-R—04/3 2004; Division of Energy and Building Design, Department of Construction and Architecture, Lund Institute of Technology: Lund, Sweden, 2004.

44. Oesterle, E.; Lieb R.D.; Lutz, M.; Heusler, W. *Double-Skin Facades Integrated Planning*; Prestel Verlag GmbH Co.KG: Munich, Germany, 2001.

45. Theodosiou, T.G. Summer period analysis of the performance of a planted roof as a passive cooling technique. *Energy Build.* **2003**, *35*, 909–917.

46. Frankenstein, S.; Koenig, G. *Fast All-Season Soil Strength (FASST)*; US Army Corps of Engineers: Washington, DC, USA, 2004.

47. Wong, N.H.; Cheong, D.K.W.; Yan, H.; Ong, C.L.; Sia, A. The effects of rooftop garden on energy consumption of a commercial building in Singapore. *Energy Build.* **2004**, *35*, 353–364.

48. Fang, C. Evaluating the thermal reduction effect of plant layers on rooftops. *Energy Build.* **2008**, *40*, 1048–1052.

49. Kim, J.; Hong, T.; Koo, C. Economic and environmental evaluation model for selecting the optimum design of green roof systems in elementary schools. *Environ. Sci. Technol.* **2012**, *46*, 8475–8483.

50. Scurlock, J.M.O.; Asner, G.P.; Gower, S.T. *Global Leaf Area Index Data form Field Measurements, 1932–2000*; Oak Ridge National Laboratory Distributed Active Archive Center: Oak Ridge, TN, USA, 2001.

51. Construction Association of Korea (CAK). *General Information for Construction*; Construction Association of Korea: Seoul, Korea, 2011.

52. Construction Association of Korea (CAK). *Monthly Construction Market Price*; Construction Association of Korea, Seoul, Korea, 2011.

53. Korea Energy Management Corporation (KEMCO). Energy Conservation Statistics. Available online: http://www.kemco.or.kr/ (accessed on 23 July 2013).

54. Korea University and College Library Association (KUCLA). Korea University and College Library Statistics. Available online: http://www.kucla.or.kr/ (accessed on 23 July 2013).

55. *DesignBuilder EnergyPlus Simulation Documentation for DesignBuilder v3.0.*; DesignBuilder Software Ltd.: Stroud, UK, 2011.

56. Crawley, D.B.; Lawrie, L.K.; Pedersen, C.O.; Winkelmann, F.C. EnergyPlus: Energy simulation program. *ASHRAE. J.* **2000**, *42*, 49–56.

57. Pappas, A.; Reilly, S. Energy Performance of a Double Skin Facade. In Proceedings of International Solar Energy Conference, Colorado, USA, 9–13 July, 2006; pp. 653–657.

58. Jiang, Q.; Long, W.D. Energy efficiency and design optimization of double-skin facade buildings. *J. HV AC* **2006**, *36*, 58–63.

59. Hashemi, N.; Fayaz, R.; Sarshar, M. Thermal behaviour of a ventilated double skin facade in hot arid climate. *Energy Build.* **2010**, *42*, 1823–1832.

60. EnergyPlus Input Output Reference. The Encyclopedic Reference to EnergyPlus Input and Output, 2010. Available online: http://www.energyplus.gov (accessed on 23 July, 2013).

61. Chen, Q.; van der Kooi, J. ACCURACY-a computer program for combined problems of energy analysis, indoor airflow, and air quality. *ASHRAE Trans.* **1988**, *94*, 196–214.

62. Zhai, Z.; Chen, Q.; Haves, P.; Klems, J.H. On approaches to couple energy simulation and computational fluid dynamics programs. *Build. Environ.* **2002**, *37*, 857–864.

63. Yu, Z.; Fung, B.; Haghighat, F.; Yoshino, H.; Morofsky, E. A systematic procedure to study the influence of occupant behavior on building energy consumption. *Energy Build.* **2011**, *43*, 1409–1417.

64. Korea Energy Management Corporation (KEMCO). Automatic Calculation of TOE and CO_2 emissions, 2009. Available online: http://co2.kemco.or.kr/ (accessed on 23 May 2013)

65. Korea Energy Management Corporation (KEMCO). *Energy and Climate Change Handbook 2010*; KEMCO: Seoul, Korea, 2010.

66. Dell'Isola, A.J.; Kirk, S.J. *Life Cycle Costing for Facilities*; Reed Construction Data: Kingston, MA, USA, 2003.

67. *Bank of Korea Economic Statistics System (ECOS)*. Available online: http://ecos.bok.or.kr/ (accessed on 30 May 2013).

68. *Korean Statistical Information Service (KOSIS)*. Available online: http://www.kosis.kr/ (accessed on 30 May 2013).

69. Korea Ministry of Knowledge Economy (KMKE). *Prime Cost Calculation Standard of Energy Service Company (ESCO) Projects*; KMKE: Seoul, Korea, 2009.